

Over-The-Air Extreme Learning Machines with XL Reception via Nonlinear Cascaded Metasurfaces

Kyriakos Stylianopoulos*, Mattia Fabiani†‡, Giulia Torcolacci†‡, Davide Dardari†‡, and George C. Alexandropoulos*

*Department of Informatics and Telecommunications, National and Kapodistrian University of Athens, 16122 Athens, Greece

†DEI, University of Bologna, 40136 Bologna, Italy

‡National Laboratory of Wireless Communications (WiLab), CNIT, 40136 Bologna, Italy

e-mails: {kstylianop, alexandg}@di.uoa.gr, {mattia.fabiani5, g.torcolacci, davide.dardari}@unibo.it

Abstract—The recently envisioned goal-oriented communications paradigm calls for the application of inference on wirelessly transferred data via Machine Learning (ML) tools. An emerging research direction deals with the realization of inference ML models directly in the physical layer of Multiple-Input Multiple-Output (MIMO) systems, which, however, entails certain significant challenges. In this paper, leveraging the technology of programmable MetaSurfaces (MSs), we present an eXtremely Large (XL) MIMO system that acts as an Extreme Learning Machine (ELM) performing binary classification tasks completely Over-The-Air (OTA), which can be trained in closed form. The proposed system comprises a receiver architecture consisting of densely parallel placed diffractive layers of XL MSs followed by a single reception radio-frequency chain. The front layer facing the MIMO channel consists of identical unit cells of a fixed NonLinear (NL) response, while the remaining layers of elements of tunable linear responses are utilized to approximate OTA the trained ELM weights. Our numerical investigations showcase that, in the XL regime of MS elements, the proposed XL-MIMO-ELM system achieves performance comparable to that of digital and idealized ML models across diverse datasets and wireless scenarios, thereby demonstrating the feasibility of embedding OTA learning capabilities into future communication systems.

I. INTRODUCTION

Future wireless networks will leverage Edge Inference (EI) to jointly train transceiver pairs as end-to-end Machine Learning (ML) models for efficient sensory data inference [1]. By exchanging task-specific representations through the channel, EI overcomes the inefficiencies of conventional decoupled designs in terms of data rate and computational burden, since feature extraction is performed alongside encoding at the Transmitter (TX), while the Receiver (RX) directly infers the target values instead of reconstructing the input data [2], [3].

To further improve computational efficiency, Over-The-Air (OTA) computing exploits the wireless propagation domain by performing computation directly through the superposition of traveling Radio-Frequency (RF) signals [4]. The OTA paradigm has recently attracted interest in wireless ML applications. Specifically, architectures based on MetaSurfaces (MSs) have been proposed to emulate Deep artificial Neural

This work has been supported by the SNS JU projects 6G-DISAC and TIMES under the EU's Horizon Europe research and innovation program under grant agreement numbers 101139130 and 101096307, respectively. The work of G. Torcolacci was funded by an NRRP Ph.D. grant.

Network (DNN) layers [2], [3], [5], [6] for OTA inference, which are trained through backpropagation. Additionally, another family of approaches uses MS-controlled channel responses to approximate digitally trained DNN weight (or similar) matrices OTA [7]–[9]. Nevertheless, many existing systems still rely on digital processing and lack theoretical foundations. Crucially, most MS-based DNN implementations are only capable of linear operations [10], which drastically reduces the approximation capability of the developed models.

Addressing some of these gaps, [11] designed an eXtremely Large (XL) Multiple-Input Multiple-Output (MIMO) system performing as an Extreme Learning Machine (ELM) [12] to execute DNN operations partially OTA, treating the channel as random hidden-layer weights and the RX analog combiner as the output layer. This approach exhibits fast training and re-tuning as the wireless channel evolves and is proven to be a universal function approximator. However, it faces practical limitations and scalability concerns due to real-valued signal constraints and hardware complexity induced by the use of NonLinear (NL) power amplifiers and numerous RF chains.

In this paper, capitalizing on the complex-domain ELM framework [13], [14] and building upon recent NL metamaterial advancements [10], [15], [16], we present an XL-MIMO-ELM system with an RX structure comprising Cascaded diffractive MSs (CMS) followed by a single antenna element and its respective RF chain. The initial MS layer facing the MIMO channel consists of unit cells of identical fixed NL responses and serves as the ELM's activation function, whereas the remaining linear MS layers perform trainable OTA combining, thereby approximating the digital ELM weights. The proposed NL-CMS-ELM system enables fast training and minimizes digital processing at the XL reception side, while significantly reducing the hardware complexity with respect to [11]'s XL-MIMO-ELM framework.

Notation: Vectors, matrices, and sets are expressed in lowercase bold, uppercase bold, and uppercase calligraphic typefaces, respectively. \mathbf{X}^\top and \mathbf{X}^H denote the transpose and conjugate transpose of \mathbf{X} . $[\mathbf{x}]_i$ is used to denote the i th element of \mathbf{x} . $|\mathcal{X}|$ represents the cardinality of the set \mathcal{X} , $\|\mathbf{X}\|_F$ denotes the Frobenius norm of \mathbf{X} , $\text{diag}(\mathbf{x})$ creates a square matrix with the elements of \mathbf{x} placed along its main diagonal. $\{\cdot\}$ expresses a set or collection, while $\mathbb{1}_{\text{cond}}$ is the indicator

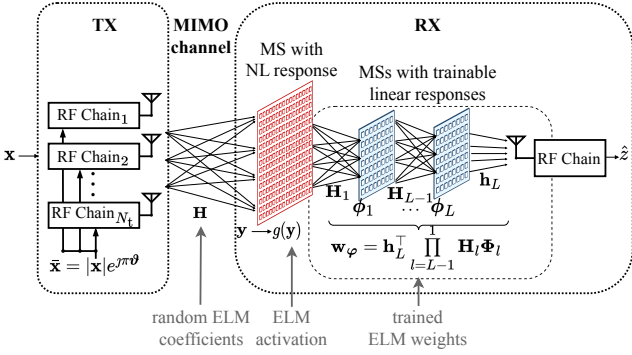


Fig. 1: The proposed XL MIMO system for implementing the proposed NL-CMS-ELM framework. Channel and MS responses are used as components of the ELM algorithm to realize OTA inference. The flow of computational during the forward pass is also sketched.

function taking value 1 if the condition `cond` holds, and 0 otherwise. Finally, $\mathbf{X} \sim \mathcal{CN}(\mathbf{0}, \sigma^2 \mathbf{I})$ signifies that \mathbf{X} follows the complex standard Gaussian distribution with variance σ^2 , $j \triangleq \sqrt{-1}$ is the imaginary unit, and $z \in \mathbb{C}$, which can be written as $z \triangleq \Re(z) + j\Im(z) = |z| \exp(j \arg\{z\})$.

II. THE PROPOSED XL MIMO SYSTEM MODEL

Consider a narrowband XL MIMO system comprising an N_t -antenna TX and an RX consisting of multiple XL diffractive MS layers with different functionalities, whose outputs are cascaded and ultimately collected by a single reception RF chain, as depicted in Fig.1. Instead of performing conventional wireless communications, the system is trained end-to-end to act as an OTA function approximator [11], [17]. In particular, given an offline dataset $\mathcal{D} \triangleq \{(\mathbf{x}^{(i)}, z^{(i)})\}_{i=1}^D$ of D input-target pairs, the XL MIMO system is designed to approximate the $\mathbf{x} \rightarrow z$ mapping so that the TX observes the input data \mathbf{x} (not necessarily belonging to \mathcal{D}) and the RX estimates its (unobserved) target value z . From this perspective, the system is intended to perform Goal-Oriented Communications (GOC) [18], with all computational processing performed exclusively OTA in the RF domain.

We assume that $\mathbf{x}^{(i)} \in [0, 1]^{N_t}$ and $z^{(i)} \in \{-1, +1\}$, i.e., the dimension of the data observations are equal to the number of TX antennas and the dataset is used for binary classification. Note that TX may introduce its own trainable feature extraction model to reduce the dimensionality of the \mathbf{x} [2], [3]; this is left for future work. For reasons that will be described later, the data points are subject to an Amplitude Modulation (AM), hence, the transmitted signal is given by the expression:

$$\bar{\mathbf{x}} \triangleq |\mathbf{x}| \exp(j\pi\vartheta) \in \mathbb{C}^{N_t \times 1}, \quad (1)$$

where the elements of ϑ may be chosen arbitrarily. The baseband representation of the signal arriving at the first (front) MS layer of the RX, which is composed of $N_r \triangleq N_r^{\text{hor}} \times N_r^{\text{vert}}$ metamaterial elements, can be expressed as follows:

$$\mathbf{y} \triangleq \mathbf{H} \bar{\mathbf{x}} \in \mathbb{C}^{N_r \times 1}, \quad (2)$$

where $\mathbf{H} \in \mathbb{C}^{N_r \times N_t}$ represent the XL MIMO channel response. For the theoretical analysis of this paper, we consider the case where \mathbf{H} follows the Rayleigh fading distribution and remains quasi-static for the duration of the training process.

A. Proposed RX Architecture

We propose an RX architecture consisting of densely parallel placed diffractive MS layers forming a CMS architecture whose purpose is to transform the impinging wave towards a single antenna element attached to a reception RF chain, as it will be explained in the following.

1) *Front MS Layer with NL Activation*: We consider the front diffractive MS layer composed of unit elements applying a memoryless NL transformation. Denoting with $F(\cdot)$ the bandpass response of the generic element of the NL MS, the baseband-equivalent output $g(\cdot)$ preserves the phase of the input while transforming its envelope through the first-order harmonic extraction. The resulting element-wise mapping of the MS is expressed as $g(\mathbf{y}) \triangleq C(|\mathbf{y}|) \exp(j\arg\{\mathbf{y}\})$, where $C(\cdot)$ denotes the AM/AM characteristic derived as [15]:

$$C(v) = \frac{2}{\pi} \int_0^\pi F(v \cos(\phi)) \cos(\phi) d\phi. \quad (3)$$

In this paper, we consider an element-wise thresholding device characterized overall by the positive bias $\mathbf{b} \in \mathbb{C}^{N_r \times 1}$, whose elements are drawn from an appropriate distribution during fabrication, hence, ensuring low complexity. From (3), the transform yields the following piecewise mapping:

$$C(|\mathbf{y}|) = \begin{cases} \mathbf{0}, & |\mathbf{y}| \leq \mathbf{b} \\ \frac{1}{\pi} \left(|\mathbf{y}| \arccos \left(\frac{\mathbf{b}}{|\mathbf{y}|} \right) \right), & |\mathbf{y}| > \mathbf{b} \\ -\mathbf{b} \sqrt{1 - \left(\frac{\mathbf{b}}{|\mathbf{y}|} \right)^2}, & \end{cases} \quad (4)$$

where all operations are applied element-wise. While this expression captures the exact physical behavior of the MS elements, the transcendental terms are computationally demanding for ELM training. By approximating the transition for $|\mathbf{y}| > \mathbf{b}$ as a linear slope, $g(\mathbf{y})$ implements a rudimentary magnitude-dependent Rectified Linear Unit (ReLU) activation function with the inclusion of the bias term. Consequently, the activation function for our system model is approximated as:

$$g(\mathbf{y}) \simeq \frac{1}{2} \max(\mathbf{0}, |\mathbf{y}| - \mathbf{b}) \exp(j\arg\{\mathbf{y}\}), \quad (5)$$

where \mathbf{b} serves as the effective hardware-induced threshold vector that facilitates NL processing in the RF domain. In [15], a possible practical implementation based on diodes is proposed. We note that an analytical activation named “modReLU”, closely resembling (5), has been used in the context of complex-valued DNNs in [19] and follow-up works.

2) *Cascade of MSs with Trainable Linear Responses*: The outputs of the front diffractive NL MS layer are then passed to a cascade of L diffractive linear MSs. Each layer comprises a square grid of N_l elements ($l = 1, 2, \dots, L$) spaced by $\lambda/2$, with $\lambda = c/f_0$ denoting the wavelength at the carrier frequency f_0 , and c is the speed of light. Let $\mathbf{H}_l \in \mathbb{C}^{N_l \times N_{l-1}}$ denote the signal propagation coefficients between the $(l-1)$ -th and the l -th MS layer, where $N_0 = N_r$ indicates the number of elements of CMS's front MS layer, and $\mathbf{h}_L \in \mathbb{C}^{N_L \times 1}$ represent the propagation between the last MS layer and the single antenna element attached to the RX RF chain. Typical works utilizing the technology of stacked intelligent metasurfaces (SIM) [20] assume free-space propagation between the MS layers, i.e., considering an anechoic enclosure, and model the element-to-element propagation through geometric optics [5], [7], [20]. In this work, we model each \mathbf{H}_l as a full rank pseudo-random matrix, which implies a reverberating enclosure around the layers [21], [22]. Arguably, this choice is more realistic as it accounts for multipath components arising from imperfections of the enclosure and allows for the MS layers to be placed arbitrarily close. Moreover, the richer propagation diversity compared to geometric optics provides substantial gains for the optimization framework, as explained in the following section.

The responses of each l -th MS layer are expressed as $\phi_l \triangleq \alpha_l \exp(j\pi\theta_l)$, with the amplitudes $\alpha_l \in [0, 1]^{N_l \times 1}$ and the phase shifts $\theta_l \in [0, 1]^{N_l \times 1}$ being *controllable* parameters. By defining $\Phi_l \triangleq \text{diag}(\phi_l)$ and $\varphi \triangleq \{\phi_l\}_{l=1}^L$, the overall transfer function of the L cascaded linear MSs is given by:

$$\mathbf{w}_\varphi \triangleq \mathbf{h}_L^\top \prod_{l=L-1}^1 \Phi_l \mathbf{H}_l \in \mathbb{C}^{1 \times N_r}. \quad (6)$$

Consequently, the signal at the output of the RX RF chain is:

$$\hat{z} \triangleq \mathbf{w}_\varphi g(\mathbf{y}) + \tilde{n}, \quad (7)$$

where $\tilde{n} \sim \mathcal{CN}(0, \sigma^2)$ represents the Additive White Gaussian Noise (AWGN).

III. TRAINING AS AN EXTREME LEARNING MACHINE

The previously presented XL MIMO system may be regarded as an affine transformation of the input (through expression (2) and the bias term in (5)) followed by the NL activation inside (5) and the final (linear) weighted sum through the cascaded response of the K linear MS layers described in (7). Subsequently, the performed computations are equivalent to those of a single-hidden-layer feedforward neural network, which motivates its deployment as a function approximator. Nevertheless, not all components are controllable. The channel responses, \mathbf{H} and \mathbf{H}_l 's, and the activation biases \mathbf{b} , in particular, are treated as random coefficients. In that regard, we leverage the ELM mathematical framework [11]–[13] used for ML inference, which allows random parameters alongside trainable weights, enabling both the training procedure and its theoretical guarantees to be rigorously described.

Algorithm 1 Training of the Proposed NL-CMS-ELM

- 1: **Inputs:** Dataset $\mathcal{D} = \{(\mathbf{x}^{(i)}, z^{(i)})\}_{i=1}^D$, TX-RX channel \mathbf{H} , MS propagation coefficients $\{\mathbf{H}_l\}_{l=1}^L$ and \mathbf{h}_L .
- 2: **for** $i = 1, \dots, D$ **do**
- 3: Construct transmit signal $\bar{\mathbf{x}}^{(i)}$ via (1).
- 4: Transmit $\bar{\mathbf{x}}^{(i)}$ to obtain $\mathbf{y}^{(i)}$ at front MS layer via (2).
- 5: Obtain $g(\mathbf{y}^{(i)})$ via the activation of (5).
- 6: **end for**
- 7: Collect all activations in \mathbf{G} via (8).
- 8: Compute ideal weights \mathbf{w}^* via (10).
- 9: Apply PGD on (11) to obtain φ^* .
- 10: **return** φ^*

In approximating the $\mathbf{x} \rightarrow z$ mapping based on \mathcal{D} , we define the ELM activation matrix $\mathbf{G} \in \mathbb{C}^{D \times N_r}$ as the transpose of the activated signals at the RX's front MS layer:

$$\mathbf{G} \triangleq [g(\mathbf{y}^1), \dots, g(\mathbf{y}^D)]^\top. \quad (8)$$

By further denoting the vector of target values for the whole dataset as $\mathbf{z} \triangleq [z^1, \dots, z^D]^\top \in \mathbb{C}^{D \times 1}$, the cascaded response of the L linear MSs, \mathbf{w}_φ , can be optimized to minimize the Least Squares (LS) error between the target and output values, following the standard ELM formulation, as follows:

$$\mathbf{w}^* \triangleq \arg \min_{\mathbf{w}_\varphi} \|\mathbf{z} - \mathbf{G}\mathbf{w}_\varphi\|_2^2. \quad (9)$$

This yields the closed-form solution:

$$\mathbf{w}^* = (\mathbf{G}^\top \mathbf{G} + \ell \mathbf{I})^{-1} \mathbf{G}^\top \mathbf{z} \in \mathbb{C}^{N_r \times 1}, \quad (10)$$

which accounts for Tikhonov regularization, controlled by the hyperparameter $\ell > 0$, to ensure generalization beyond the training dataset \mathcal{D} .

While (10) provides a fast and convenient way to determine the cascaded MS response, \mathbf{w}_φ is not directly controllable because of the physical limitations introduced by the diffractive MSs. Instead, the trainable parameters are α_l 's and θ_l 's of φ . Therefore, as the second step of our training approach, we take inspiration from works that use MS responses to approximate arbitrary matrices, including DNN weights [7]–[9], and we choose to find appropriate φ values that approximate \mathbf{w}^* as:

$$\varphi^* = \{\phi_l^*\}_{l=1}^L \triangleq \arg \min_{\mathbf{w}_\varphi, \rho} \|\mathbf{w}^* - \rho \mathbf{w}_\varphi^\top\|_F, \quad (11)$$

where $\rho > 0$ is a scaling term to compensate for the inadvertent signal attenuation induced by (6). In practice, this implies the inclusion of dedicated amplification at the single reception RF chain (e.g., via the low noise amplifier). Since (6) provides an analytic expression for \mathbf{w}_φ , (11) is differentiable with respect to α_l and θ_l . Consequently, the minimization is performed via Projected Gradient Descent (PGD) by projecting α_l , θ_l , and ρ onto their respective feasible sets. The overall training procedure is summarized in Algorithm 1, while the use of the trained system for inferring a target value given an input data point is detailed in Algorithm 2.

Algorithm 2 Inference with the Proposed NL-CMS-ELM

- 1: **Inputs:** Inference data point \mathbf{x} , TX-RX shannel \mathbf{H} , MS propagation coefficients $\{\mathbf{H}_l\}_{l=1}^L$ and \mathbf{h}_L , MS weights φ^* .
- 2: **for** $i = 1, \dots, L$ **do**
- 3: Set $\phi_l = \phi_l^*$ to the l -th MS.
- 4: **end for**
- 5: Construct transmit signal $\bar{\mathbf{x}}$ via (1).
- 6: Transmit $\bar{\mathbf{x}}$ to obtain \mathbf{y} at front MS layer via (2).
- 7: Obtain $g(\mathbf{y})$ via the activation of (5).
- 8: Obtain inferred value \hat{z} at the RX RF chain via (7).
- 9: **return** \hat{z}

A. Theoretical Analysis

Notwithstanding the inclusion of random coefficients, the ELM framework has been proven to be a universal approximator [12], [14]. To showcase the same property for the proposed NL-CMS-ELM approach via the XL MIMO system described in Section II, we list the necessary assumptions as below:

- 1) *Rich scattering*: Assume that the TX-RX channel \mathbf{H} and the intra-layer channels \mathbf{H}_l 's are characterized by uncorrelated rich scattering conditions, indicating strong multipath or reverberation enclosures, respectively.
- 2) *Static fading*: Assume \mathbf{H} remains quasi-static for the duration of the training and inference process. The validity, implications, and mitigation for this assumption are further discussed in the following.
- 3) *XL MIMO regime*: Assume N_r can be arbitrarily large. It is noted that, since N_r also corresponds to the number of unit cells at the front MS layer of the RX, and not to the number of the reception RF chains, it is reasonable to expect MSs with hundreds to thousands of elements in future wireless networks.

Leveraging the above assumptions, we express the following conditions for universal approximation:

Condition 1. (Denseness of the affine projection) *The affine transformation applied via the combination of the channel response of (2) and the bias term of (5) is dense in $\mathbb{C}_+^{N_r}$.*

Proof. Under rich scattering conditions, $|\mathbf{H}|$ follows an uncorrelated Rayleigh distribution and $\arg\{\mathbf{H}\}$ follows a uniform distribution, making \mathbf{H} a full-rank matrix almost surely in the asymptotic limit. Additionally, the bias term \mathbf{b} can be sampled by any distribution with infinite support. Since the considered distributions have infinite support over \mathbb{C}_+ , the overall transformation is dense in $\mathbb{C}_+^{N_r}$. \square

Condition 2. (Discriminatory activation) $g(y) : \mathbb{C} \rightarrow \mathbb{C}$ of (5) is a continuous discriminatory function [17].

Proof. Following [23], it suffices to show that $g(\cdot)$ is a locally bounded piecewise continuous non-polynomial function. While the results of [23] consider real-valued functions, the work of [24] demonstrated that they hold for complex-valued functions by treating \mathbb{C} as isomorphic to \mathbb{R}^2 . First, $g(\cdot)$ is locally bounded since it is continuous in \mathbb{C} . Additionally, $g(y)$ is not polynomial as: *i*) it has a constant value of 0 in the

open region $|y| < b$ without being 0 everywhere, where b is the scalar bias substituting \mathbf{b} in (5); and *ii*) it involves the non-polynomial expression $|y| \triangleq \sqrt{\Re(y)^2 + \Im(y)^2}$. \square

We can thus express the universal approximation property for our proposed NL-CMS-ELM framework:

Proposition 1. *Consider the NL-CMS-ELM expressed via (7) and the aforementioned assumptions and conditions. There exists $N_r \leq D$ such that, for D arbitrary distinct samples of $\mathcal{D} = \{(\mathbf{x}^{(i)}, z^{(i)})\}_{i=1}^D$, there exists $\mathbf{w}^* \in \mathbb{C}^{N_r \times 1}$ so that $\|\mathbf{z} - \mathbf{G}\mathbf{w}^*\| < \epsilon$ for arbitrarily small ϵ with probability 1.*

Proof. The proof follows the direct application of [14, Theorem 3.1] with a change of notation. \square

It is noted that, in practice, the effectiveness of the approximation depends additionally on the successful approximation of \mathbf{w}^* with \mathbf{w}_φ via (11). Assumption 1 ensures that each \mathbf{H}_l included in (6) is almost surely a full-rank matrix, therefore aiding in the approximation of arbitrary values of \mathbf{w}^* .

B. Computational Complexity

The time complexity for obtaining the solution of (9) is $\Theta(DN_r \min\{D, N_r\})$, stemming from the matrix inversion of (10). For reasonably small datasets with XL MIMO systems where $D = \Theta(N_r)$, the complexity reduces to $\Theta(N_r^3)$, which is equivalent to typical MIMO decoding operations (such as zero forcing and weighted mean square error) and, therefore, may be computed within a channel coherence frame. The time complexity of the gradient descent solution of (11) is $\Theta(TN_rLN_{\max}^2)$, which can be reduced to $\Theta(TL)$ assuming appropriate parallel hardware, where T is the number of iterations until convergence and $N_{\max} \triangleq \max\{N_1, \dots, N_L\}$. Considering the assumption of large N_r values, the convergence of the gradient is not practically fast enough to be implemented within a single channel coherence block. However, it does not depend on the size of the dataset, which offers a remarkable computational improvement over typical backpropagation-based learning of DNNs. Importantly, the recent work [11] demonstrated that, when the channel exhibits correlated fading, only a low complexity re-training of the XL-MIMO-ELM architecture is necessary, since the optimal weights change marginally. It is therefore feasible to re-tune such models as the channel changes. We defer the adoption of such techniques for our NL-CMS-ELM framework to the journal version of this work due to a lack of space.

IV. NUMERICAL RESULTS AND DISCUSSION

We perform investigations on the performance of the proposed NL-CMS-ELM over a number of standard binary classification datasets of small-to-medium size under a variety of system conditions. The considered datasets [25] are the Parkinson's and the Wisconsin Breast Cancer Dataset (WBCD) of 22 and 30 numerical features for disease diagnosis, respectively, as well as the MNIST dataset of handwritten digit image recognition [26]. Due to the large dimensionality of the latter dataset, we have subsampled 100 pixels from the images at

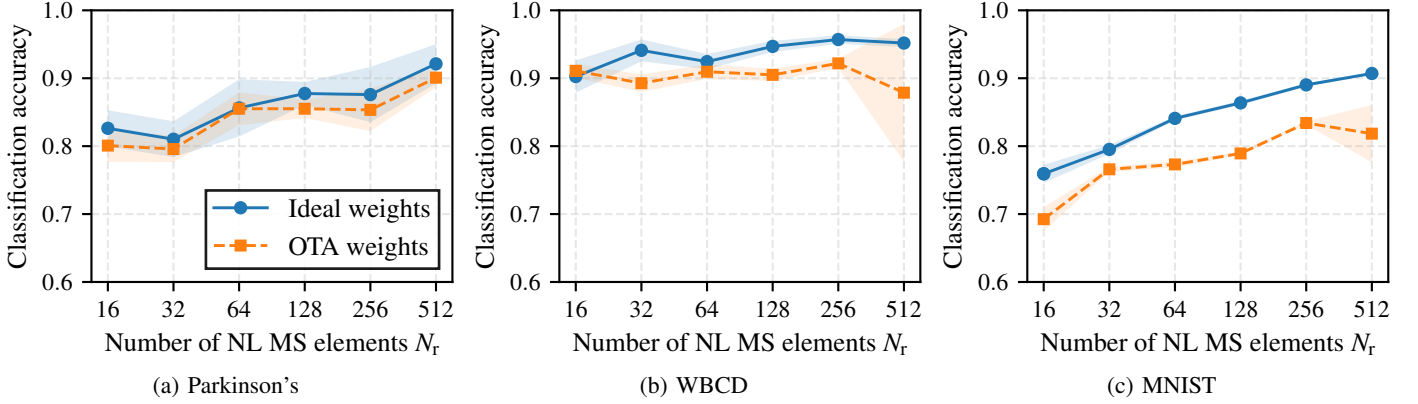


Fig. 2: Classification accuracy of two NL-CMS-ELM variations versus the number of elements N_r at the RX's front MS layer, which corresponds to the number of ELM trainable parameters for three distinct datasets. The “ideal weights” variation assumes the ELM weights are applied in the digital domain or under idealized analog hardware. The “OTA weights” variation approximates those weights through L cascaded MSs with linear responses for full OTA inference.

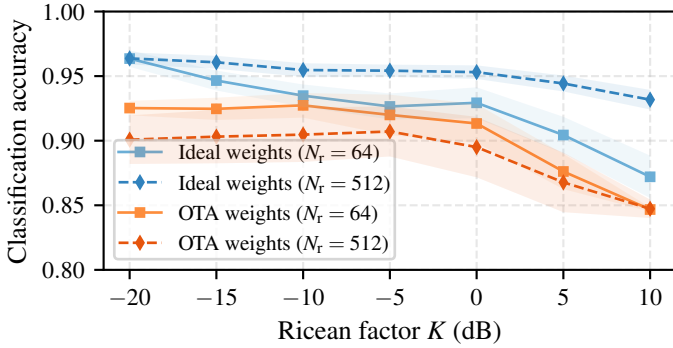


Fig. 3: Classification accuracy of two NL-CMS-ELM variations over different Ricean factors for the WBCD dataset, considering different values N_r for the RX's front MS layer.

random locations to define the input features. To convert this dataset into a binary classification one, we have assumed that the two classes correspond to even and odd digits, respectively.

For pre-processing, all features have been independently scaled to $[0, 1]$. As explained in Section II, the input features are encoded in the amplitudes of the transmitted signal vector, following an AM transmission scheme. Consequently, the classification decision based on the output of the system through (7) is expressed as $\hat{c} = \mathbb{1}_{\Re(z) > 0.5}$ and the classification accuracy, used as our evaluation metric, was measured as $\sum_{i=1}^{|D'|} \mathbb{1}_{\Re(z^{(i)}) = \hat{c}^{(i)}} / |D'|$ for each of the test sets D' , which have been created via a 70 : 30 split in the data points. In our XL MIMO system, N_t is determined by the number of features in the datasets, and we have varied the values of N_r to investigate performance scaling. Unless otherwise specified, $\mathbf{H} \sim \mathcal{CN}(\mathbf{0}, P_L \mathbf{I})$, where P_L is the pathloss set to -50 dB. The phases ϑ of the AM signals were set to 0 for all data points. Similarly, we have sampled \mathbf{b} from a Rayleigh distribution with scale parameter $\mathbb{E}[\|\mathbf{H}\|_F] / (2N_r N_t)$ for the biases to be in the same order as $|\mathbf{y}|$. Since z contains only

1 bit of information, we have set the receive Signal-to-Noise Ratio (SNR) to a moderate level of 15 dB in order to assess the performance without severe noise degradation. A validation under different SNR levels and erroneous system information will be included in the journal version. We have used $L = 5$ linear MS layers, each consisting of $N_l = 64 \times 64$ diffractive elements. Similarly, we considered $\mathbf{H}_l \sim \mathcal{CN}(\mathbf{0}, P'_L \mathbf{I})$ with P'_L set to -10 dB. Finally, we set the regularization weight $\ell = 10^{-6}$ to avoid severe overfitting, and we allowed a maximum of $T = 1500$ iterations of the employed PGD procedure with step size 0.01, although convergence was achieved far earlier for most scenarios.

Two main variations of the proposed NL-CMS-ELM system were investigated. The first one, referred to as “OTA weights,” implements Algorithms 1 and 2, where linear MSs are used to approximate \mathbf{w}^* OTA. We also considered the idealized case where the optimal weight vector is used directly to compute the output as $\hat{z} = (\mathbf{w}^*)^\top g(\mathbf{y})$, instead of (7). This approach, referred to as “ideal weights,” considers the RX's CMS structure with only the front NL MS layer (i.e., $L = 0$), whose N_r outputs are guided to be multiplied with the \mathbf{w}^* elements. This idealized weighting can be realized either with digital (requires N_r RF chains) or analog (a single RF chain suffices) combining. For the latter option, phase shifters as in [11] or an MS structure as in [27] with lossless waveguides can be used. Moreover, we report that a 3-layer fully connected DNN trained on the considered datasets achieved 92%-98% classification accuracy, which constitutes an upper bound. The trained ELMs with the same number of trainable parameters as the N_r values, in every case, achieved similar performance to the NL-CMS-ELMs, and are thus omitted for clarity.

The performance of the two considered NL-CMS-ELM variations for an increasing number of elements N_r at the RX's front MS layer is displayed in Fig. 2. It is noted that the values of N_r also represent the number of ELM trainable parameters, which affects the capacity of the considered models in solving the classification problems. As observed, in all cases, the

classification accuracy increases as N_r increases, approaching the upper bounds provided by the theoretical DNN benchmarks in the largest XL MIMO cases. It is also shown that the approximation offered by the linear MS layers exhibits close performance to the ELM approach using the ideal weights, although, for the largest N_r values, a noticeable performance degradation occurs due to insufficient PGD convergence.

Finally, we have assumed pure Rayleigh conditions in the TX-RX channel, implying that \mathbf{H} becomes full-rank, a fact that aids in the universal approximation properties of the NL-CMS-ELM. For the results reported in Fig. 3, we have relaxed this condition to sample channel matrices from a Ricean model [28] in increasing Line-of-Sight (LoS) conditions, defined as:

$$\mathbf{H} = \sqrt{P_L} \left(\sqrt{\frac{K}{1+K}} \mathbf{H}_{\text{LoS}} + \sqrt{\frac{1}{1+K}} \mathbf{H}_{\text{NLoS}} \right), \quad (12)$$

where \mathbf{H}_{LoS} is a rank-1 matrix of steering vectors, $\mathbf{H}_{\text{NLoS}} \sim \mathcal{CN}(\mathbf{0}, 1/\sqrt{N_t N_r} \mathbf{I})$, and K is the Ricean factor that controls the dominance of either component. Figure 3 indicates that the NL-CMS-ELMs have a steady performance when the channel is sufficiently diverse. However, as the channel becomes LoS-dominant, the classification accuracy decreases, since the conditions for the universal approximation cease to hold.

V. CONCLUSION

This work showcases that XL MIMO systems with purposely designed MS components at the RX side can perform computations that are akin to a complex-valued ELM model, and can thus be used to perform ML-based inference on the data the TX transmits completely OTA. Based on rich scattering conditions, the channel coefficients are treated as random weights of the XL-MIMO-ELM's hidden layer, while the RX's CMS, comprising a diffractive MS with pseudorandom NL response and multiple diffractive MSs with trainable linear responses, followed by a single reception RF chain provides the activation function and bias directly in the RF domain. The linear MSs are also utilized to approximate OTA the optimal trainable ELM weights. A two-step training approach is presented for the proposed NL-CMS-ELM approach, together with an investigation into the framework's universal approximation properties. The presented numerical investigation demonstrated classification performance approaching digital ML models in the XL MIMO regime, while resilience to channel diversity levels was also shown.

REFERENCES

- [1] A. Li, S. Wu, S. Meng, R. Lu, S. Sun, and Q. Zhang, "Toward goal-oriented semantic communications: New metrics, framework, and open challenges," *IEEE Wireless Commun.*, vol. 31, no. 5, pp. 238–245, 2024.
- [2] G. Huang, J. An, Z. Yang, L. Gan, M. Bennis, and M. Debbah, "Stacked intelligent metasurfaces for task-oriented semantic communications," *arXiv preprint arXiv:2407.15053*, 2024.
- [3] K. Stylianopoulos, P. Di Lorenzo, and G. C. Alexandropoulos, "Over-the-air edge inference via metasurfaces-integrated artificial neural networks," *arXiv preprint arXiv:2504.00233*, 2025.
- [4] A. Şahin and R. Yang, "A survey on over-the-air computation," *IEEE Commun. Surveys & Tuts.*, vol. 25, no. 3, pp. 1877–1908, 2023.
- [5] X. Lin, Y. Rivenson, N. T. Yاردیمci, M. Veli, Y. Luo, M. Jarrahi, and A. Ozcan, "All-optical machine learning using diffractive deep neural networks," *Science*, vol. 361, no. 6406, pp. 1004–1008, 2018.
- [6] A. Momeni and R. Fleury, "Electromagnetic wave-based extreme deep learning with nonlinear time-floquet entanglement," *Nature Commun.*, vol. 13, no. 1, p. 2651, May 2022.
- [7] J. An, C. Yuen, Y. L. Guan, M. Di Renzo, M. Debbah, and H. V. Poor, "Stacked intelligent metasurface performs a 2D DFT in the wave domain for DOA estimation," in *Proc. IEEE Int. Commun. Conf.*, Denver, USA, 2024.
- [8] M. Hua, C. Bian, H. Wu, and D. Gündüz, "Implementing neural networks over-the-air via reconfigurable intelligent surfaces," *arXiv preprint arXiv:2508.01840*, 2025.
- [9] M. E. Pandolfo, K. Stylianopoulos, G. C. Alexandropoulos, and P. Di Lorenzo, "Over-the-air semantic alignment with stacked intelligent metasurfaces," *arXiv preprint arXiv:2512.05657*, 2025.
- [10] K. Stylianopoulos, M. E. Pandolfo, P. Di Lorenzo, and G. C. Alexandropoulos, "Metasurfaces-integrated wireless neural networks for lightweight over-the-air edge inference," *IEEE Wireless Commun.*, under review, 2025.
- [11] K. Stylianopoulos and G. C. Alexandropoulos, "Universal approximation with XL MIMO systems: OTA classification via trainable analog combining," *arXiv preprint arXiv:2504.12758*, 2025.
- [12] G.-B. Huang, Q.-Y. Zhu, and C.-K. Siew, "Extreme learning machine: Theory and applications," *Neurocomput.*, vol. 70, no. 1, pp. 489–501, 2006.
- [13] M.-B. Li, G.-B. Huang, P. Saratchandran, and N. Sundararajan, "Fully complex extreme learning machine," *Neurocomput.*, vol. 68, pp. 306–314, 2005.
- [14] G.-B. Huang, M.-B. Li, L. Chen, and C.-K. Siew, "Incremental extreme learning machine with fully complex hidden nodes," *Neurocomput.*, vol. 71, no. 4, pp. 576–583, 2008.
- [15] M. Fabiani, G. Torcolacci, and D. Dardari, "Nonlinear EM-based signal processing," in *Proc. Asilomar Conf. Signals, Sys., and Comput.*, Pacific Grove, USA, 2025.
- [16] O. Abbas, A. Zayat, L. Markley, and A. Chaaban, "Nonlinear stacked intelligent surfaces for wireless systems," *arXiv preprint arXiv:2510.23780*, Oct. 2025.
- [17] G. Cybenko, "Approximation by superpositions of a sigmoidal function," *Math. Control Signal Sys.*, vol. 2, p. 303–314, 1989.
- [18] O. Goldreich, B. Juba, and M. Sudan, "A theory of goal-oriented communication," *J. Assoc. Comput. Mach.*, vol. 59, no. 2, 2012.
- [19] M. Arjovsky, A. Shah, and Y. Bengio, "Unitary evolution recurrent neural networks," in *Proc. Int. Conf. Mach. Learn.*, New York, USA, 2016.
- [20] J. An, C. Xu, D. W. K. Ng, G. C. Alexandropoulos, C. Huang, C. Yuen, and L. Hanzo, "Stacked intelligent metasurfaces for efficient holographic MIMO communications in 6G," *IEEE J. Sel. Areas Commun.*, vol. 41, no. 8, pp. 2380–2396, 2023.
- [21] R. Faqiri, C. Saigre-Tardif, G. C. Alexandropoulos, N. Shlezinger, M. F. Imani, and P. del Hougne, "PhysFad: Physics-based end-to-end channel modeling of RIS-parametrized environments with adjustable fading," *IEEE Trans. Wireless Commun.*, vol. 22, no. 1, pp. 580–595, 2023.
- [22] A. Rabault, L. Le Magorou, J. Sol, G. C. Alexandropoulos, N. Shlezinger, H. V. Poor, and P. del Hougne, "On the tacit linearity assumption in common cascaded models of RIS-parametrized wireless channels," *IEEE Trans. Wireless Commun.*, vol. 23, no. 8, pp. 10001–10014, 2024.
- [23] M. Leshno, V. Y. Lin, A. Pinkus, and S. Schocken, "Multilayer feedforward networks with a nonpolynomial activation function can approximate any function," *Neural Netw.*, vol. 6, no. 6, pp. 861–867, 1993.
- [24] F. Voigtlaender, "The universal approximation theorem for complex-valued neural networks," *Appl. Comput. Harmon. Anal.*, vol. 64, pp. 33–61, 2023.
- [25] D. Dua and C. Graff, "UCI machine learning repository," University of California, Irvine, School of Information and Computer Sciences, 2017. [Online]. Available: <http://archive.ics.uci.edu/ml>
- [26] L. Deng, "The MNIST database of handwritten digit images for machine learning research," *IEEE Signal Process. Mag.*, vol. 29, no. 6, pp. 141–142, 2012.
- [27] N. Shlezinger, G. C. Alexandropoulos, M. F. Imani, Y. C. Eldar, and D. R. Smith, "Dynamic metasurface antennas for 6G extreme massive mimo communications," *IEEE Wireless Commun.*, vol. 28, no. 2, pp. 106–113, 2021.
- [28] M. Matthaiou, G. C. Alexandropoulos, H. Q. Ngo, and E. G. Larsson, "Analytic framework for the effective rate of MISO fading channels," *IEEE Trans. Commun.*, vol. 60, no. 6, pp. 1741–1751, 2012.